Soft Matter

www.softmatter.org

Volume 4 | Number 2 | 7 February 2008 | Pages 181–368

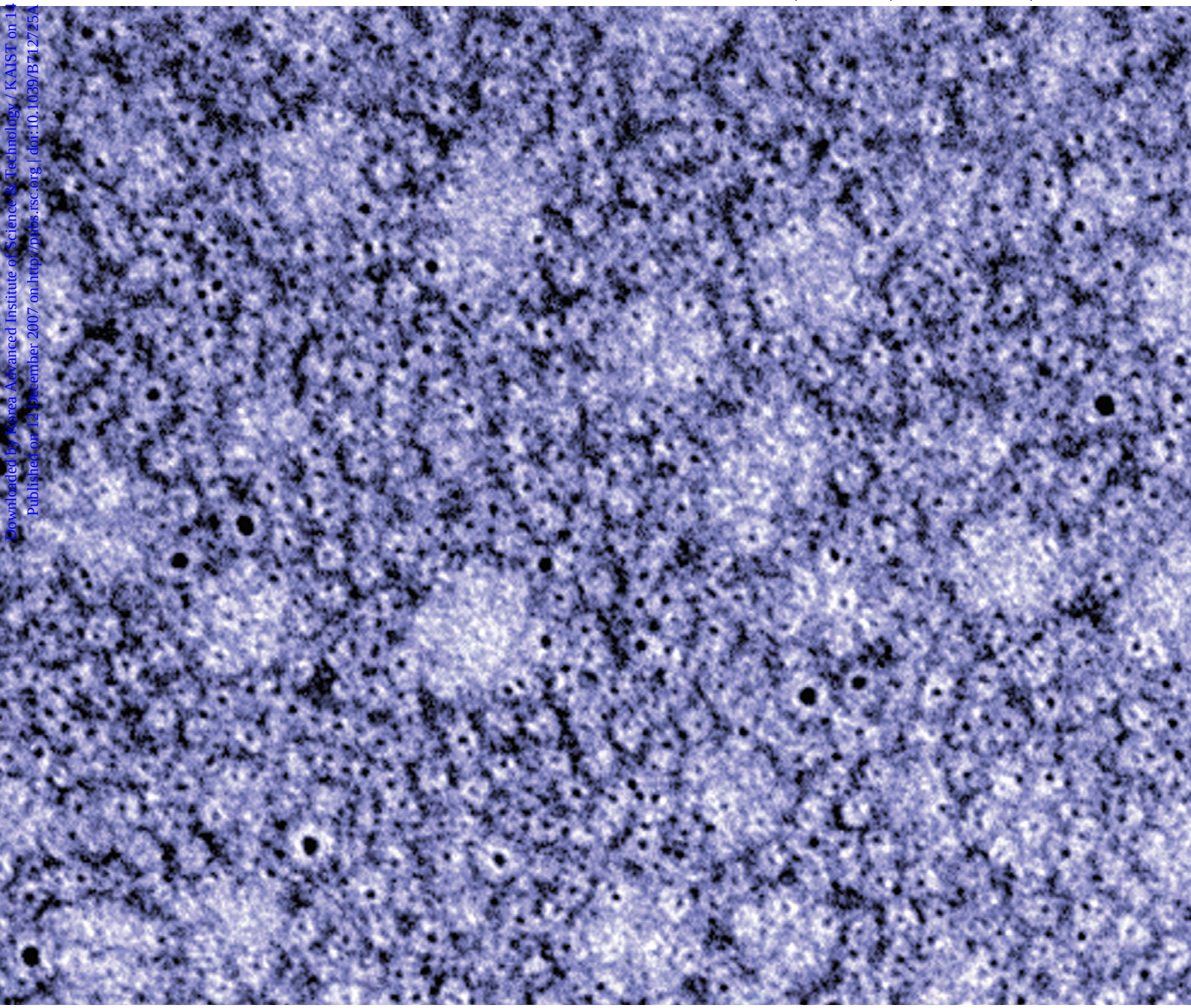

ISSN 1744-683X

RSC Publishing

Aqueous self-assembly of amphiphilic nanocrystallo-polymers and their surface-active properties†

Kwang-Suk Jang,‡[a] Hyun Jin Lee,‡[a] Hee-Man Yang,[a] Eun Jung An,[a] Tae-Hwan Kim,[b] Sung-Min Choi[b] and Jong-Duk Kim*[a]

Received 20th August 2007, Accepted 14th November 2007
First published as an Advance Article on the web 12th December 2007
DOI: 10.1039/b712725a

The self-assembly of nanocrystals using a bottom-up approach is advantageous because it is possible to control their direct structure at a nanometre length scale and their collective optical and electronic properties. Here, we present the novel fabrication and aqueous self-assembly of amphiphilic nanocrystallo-polymers. Hydrophobic nanocrystals are used as the hydrophobic component of amphiphiles, and they can drive the hydrophobic interaction-mediated direct self-assembly to create various nanostructures, such as spherical aggregates, core–shell unimolecular micelles, and cylinders. The nanocrystals can be uniformly arranged in the core of the nanostructures. We further show that the amphiphilic nanocrystallo-polymers have dynamic self-assembling and surface-active properties.

Introduction

In aqueous media, organic solvents, or a mixture of both, amphiphilic molecules self-assemble into various nanostructures such as spherical and cylindrical micelles, lamellae, and vesicles.[1–3] These self-assemblies display unique characteristics, can be utilized in a variety of applications in many fields, and have been extensively studied during the past decade. Recently, self-assemblies from metallo-surfactants or assemblies loaded with inorganic nanoparticles have been the subject of considerable attention, because they provide new functions that are not achievable with organic amphiphiles.[4–7] However, metallo-surfactants exhibit modified and restricted properties related to metal ions rather than the original metallic properties, and most nanoparticle-loaded assembly systems limit structural diversity and controllability as a result of the assembly methodologies. Here, we report on the hydrophobic interaction-mediated direct self-assembly of amphiphilic 'nanocrystallo-polymers', hydrophilic poly(amino acid) derivatives grafted with hydrophobic Au nanocrystals. Au nanocrystals protected by an alkyl chain monolayer are chemically conjugated onto a hydrophilic polymer backbone *via* a thiolate bond and these amphiphiles can direct the self-assembly into forming spherical aggregates by serving as the hydrophobic component in a nanocrystallo-polymer system. With the selective introduction of a dodecyl chain as the co-hydrophobic component, we can obtain a wide range of hydrophilic/hydrophobic compositions of nanocrystallo-polymers with multiple morphologies, *i.e.* spherical aggregates, core–shell unimolecular micelles, and cylinders, in aqueous solutions.

Recently, the self-assembly of oligomer-functionalized nanoparticles with diverse morphologies has been predicted by simulation studies[8,9] and discrete self-aggregates of nanocrystals with polymer matrix using a 'bricks and mortar' method or with template of block copolymers with self-assembling properties.[10–13] The present study has a number of advantages over previous methods. Since conjugated nanocrystals are the hydrophobic component of amphiphiles, they have dynamic self-assembling and surface-active properties. Therefore, the self-assembling process is simple, diverse morphologies can be obtained, and the arrangement of nanocrystals is more regular and controllable.

Results and discussion

Au nanocrystals and a polymer backbone containing Au nanocrystal-linkable side chains were prepared. Poly(2-hydroxyethyl L-aspartamide) (PHEA), a water-soluble biocompatible polymer with a poly(amino acid) structure, can be prepared from poly(succinimide) (PSI) and can be easily modified to form graft structures.[14,15] The molecular weight (M_n) of PHEA determined by gel permeation chromatography (GPC) was 19 800 (PDI = 1.32).[16] We prepared PHEA conjugated with undecanethiols (P-*g*-C_{11}SH) by forming an ester bond between PHEA and an 11-mercaptoundecanoic acid as shown in Fig. 1a. The synthesis was verified with ^{1}H NMR spectra (see ESI 1†), and the grafted mole percent, defined as the degree of substitution (DS) in the graft polymer system, for the undecanethiol groups was calculated to be 2.92 mol% (Table 1). Conjugated undecanethiols serve as a link between PHEA and the Au nanocrystals. Dodecanethiolate-protected Au nanocrystals were prepared

[a]*Department of Chemical and Biomolecular Engineering (BK21 Graduate Program), Korea Advanced Institute of Science and Technology, Daejeon 305-701, Republic of Korea. E-mail: jdkim@kaist.ac.kr*
[b]*Department of Nuclear and Quantum Engineering, Korea Advanced Institute of Science and Technology, Daejeon 305-701, Republic of Korea*

† Electronic supplementary information (ESI) available: ^{1}H NMR spectra, synthetic procedure, small-angle XRD pattern, description of surface-active properties, and AFM images. See DOI: 10.1039/b712725a

‡ These authors contributed equally to this work.

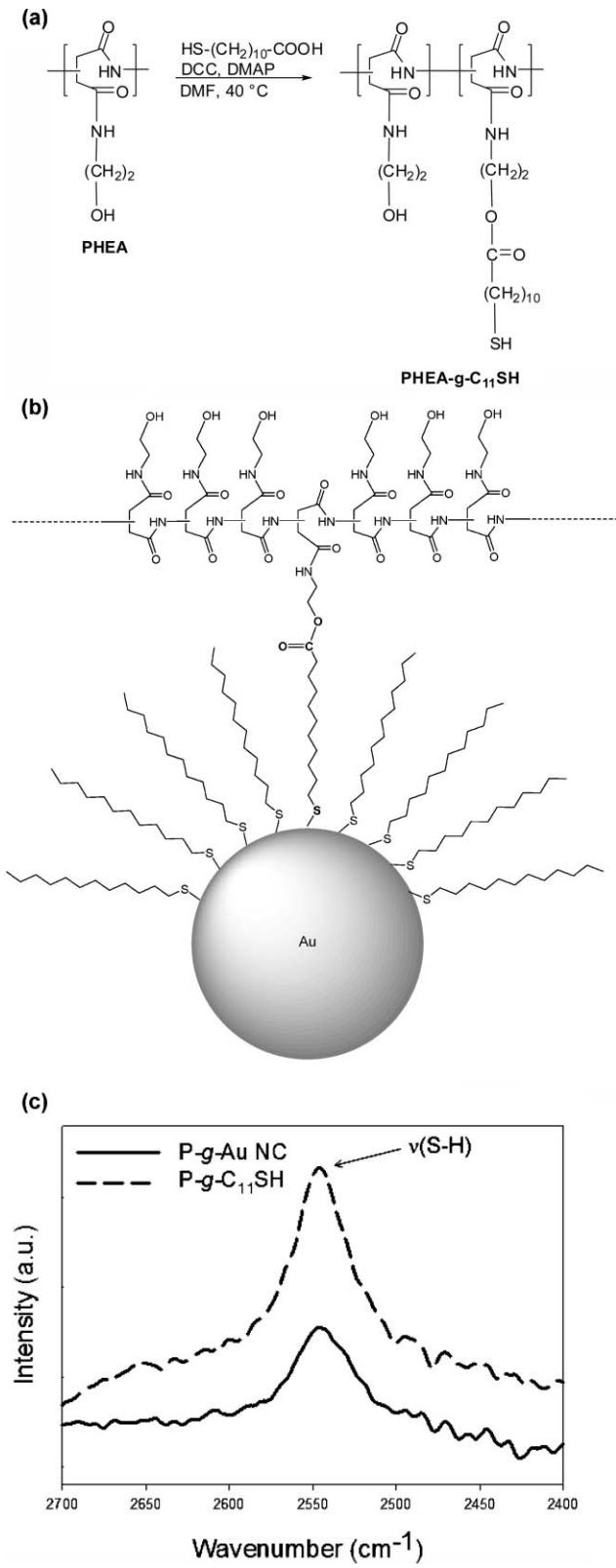

Fig. 1 Synthetic route of amphiphilic nanocrystallo-polymer. (a) PHEA grafted with undecanethiols. (b) PHEA grafted with dodecanethiolate-protected Au nanocrystals. (c) Raman spectra of the ν(S–H) region for precursor polymer, P-*g*-C_{11}SH, and nanocrystallo-polymer, P-*g*-Au NC.

using the Brust–Schiffrin method,[17–19] and it was confirmed *via* TEM analysis that they had a 1.5 nm average core diameter (see ESI 2†). The alkanethiol ligands were strongly bound to the gold surface due to the soft character of both Au and S.[17–20] Therefore, the dodecanethiolate monolayer offers a stable hydrophobic surface, and the Au nanocrystals are soluble in appropriate organic solvents without irreversible aggregation or decomposition.

The alkanethiolate monolayer reacts with other thiolate ligands to induce ligand place-exchange.[21–24] Ligand place-exchange is a key step in the formation of the amphiphilic nanocrystallo-polymers. Undecanethiols conjugated onto PHEA can participate in ligand place-exchange to form PHEA grafted with alkanethiolate-protected Au nanocrystals (P-*g*-Au NC), as described in Fig. 1b. We have named this polymer ''nanocrystallo-polymer''. The P-*g*-Au NC was prepared as follows. P-*g*-C_{11}SH was dissolved in DDI water and Au nanocrystals were dissolved in tetrahydrofuran (THF). The Au nanocrystal–THF solution was added dropwise to the polymer–water solution under vigorous stirring, and the mixture was stirred continuously for 1 day to achieve ligand place-exchange. By removing the THF and unreacted Au nanocrystals, the nanocrystallo-polymer forming nanocrystallo-aggregates in the aqueous solution was prepared. It was calculated that two polymer chains were conjugated to one Au nanocrystal on average. The weight% of Au in dodecanethiol-protected Au nanocrystals measured by thermal gravimetric analysis (TGA) was 75% and the atomic weight% of Au in P-*g*-Au NC determined by inductively coupled plasma atomic emission spectrometer (ICP-AES) was 18.8%. In order to confirm that the Au nanocrystals were chemically linked to the polymer backbone, the information regarding the chemical bonds was analyzed using Raman spectroscopy. The reduction of the characteristic band of the S–H bond at 2546 cm^{-1} verifies the covalent attachment of the Au nanocrystals to the PHEA backbone *via* cleavage of the S–H bond (Fig. 1c).[25] As shown in Fig. 2a, the original Au nanocrystals are soluble in a hydrophobic solvent such as chloroform, but the self-aggregates of the nanocrystallo-polymer are stable in water and do not proceed to the oil phase. To prove that the nanocrystallo-polymer is a surface-active amphiphile forming self-assembled nanostructures in aqueous media, for the conjugated Au nanocrystals were a hydrophobic component, the surface tension was measured. The surface activity of water-soluble materials is correlated and often evaluated with their capacity to reduce the surface tension of water. Fig. 2b shows the surface tension of the aqueous solution of nanocrystallo-polymer, P-*g*-Au NC, as a function of concentration. The surface tension decreases with the increase of nanocrystallo-polymer concentration indicating the accumulating adsorption of the nanocrystallo-polymers at the water surface with the hydrophilic PHEA backbones pointing towards the water and the hydrophobic Au nanocrystals towards the air. This arrangement lowers the interfacial free energy per unit area and is commonly characterized by the surface tension. By analogy with surfactants and amphiphilic block copolymers, the critical aggregation concentration (CAC) was observed and determined to be 0.075 g L^{-1}, which is of the order of 10^{-6} mole and a typical value for amphiphilic

Table 1 Molecular characterization results of PHEA grafted with undecanethiols and dodecyl chains and formed nanocrystallo-polymers

Precursor polymer	DS_{C11SH} (mol%)	DS_{C12} (mol%)	Nanocrystallo-polymer	A_{510nm}[a]	Self-assembled structures
P-*g*-C_{11}SH	2.92	0	P-*g*-Au NC	3.5	Spherical aggregate
P-*g*-C_{11}SH-C_{12} 1	3.01	6.27	P-*g*-Au NC-C_{12} 1	3.8	Spherical aggregate
P-*g*-C_{11}SH-C_{12} 2	3.01	18.5	P-*g*-Au NC-C_{12} 2	3.7	Core-shell unimolecular micelle
P-*g*-C_{11}SH-C_{12} 3	3.01	24.0	P-*g*-Au NC-C_{12} 3	4.2	Cylinder

[a] Light absorbance at 510 nm in the concentration of 5 mg mL^{-1} (nanocrystallo-polymer/DDI water)

block copolymers. Above the CAC, the surface tension remained constant at approximately 40 mN m^{-1} because the surface adsorption became saturated and self-assembled aggregates were formed in the solution. The nanocrystallo-polymers with Au nanocrystals as the only hydrophobic component had high surface activity and their self-assemblies were derived from the surface-active properties.

Fig. 3a and 3b show the TEM images of the spherical aggregates formed from P-*g*-Au NC in aqueous solution. Hydrophobic Au nanocrystals are tightly packed inside a self-aggregate to form a core, and hydrophilic PHEA should be located at the surface of the core part to form a corona layer. Only the core parts filled with close-packed Au nanocrystals were observed due to the very high electron density of metals, while the organic corona layer is not visible in the TEM. Uniformly close-packed nanocrystals in the core of the spherical aggregates were confirmed by a small-angle X-ray diffraction (XRD) pattern (see ESI 3†). The *d*-spacing was calculated to be 3.083 nm which is the average inter-nanocrystal distance in the core section of the aggregates. This corresponds well to the TEM image of the nanocrystallo-spherical aggregates. The hydrodynamic mean diameter (D_h) of the aggregates measured by dynamic light scattering (DLS) was 89.5 nm. This is larger than the value observed in the TEM images (20–70 nm) because the sampling and observation process for TEM is processed in a dry condition *in vacuo* and the organic corona layer is not observed in the TEM images. The spherical-shaped aggregates were formed by direct self-assembly of the amphiphilic nanocrystallo-polymer, itself, as a nano-building block of the supramolecular aggregates. Even though the hydrophobic parts were not organic chains but rather much more bulky and dense inorganic nanocrystals, the amphiphiles self-assemble into spherical aggregates by the strong hydrophobic interactions among the Au nanocrystals in the aqueous solution.

Using other types of inorganic nanocrystals with hydrophobic and place-exchangeable ligands, self-assembling amphiphilic nanocrystallo-polymers could be fabricated. We

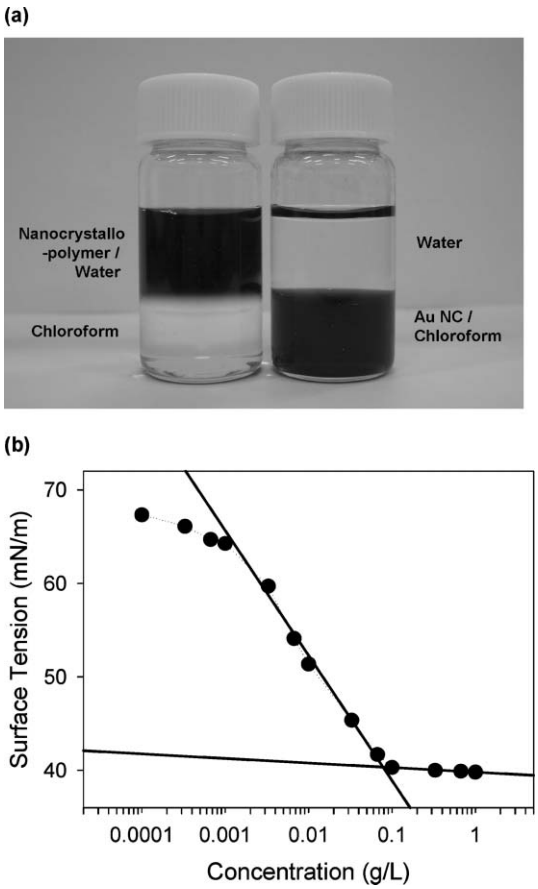

Fig. 2 Amphiphilic properties of PHEA grafted with Au nanocrystals. (a) Water solution of nanocrystallo-polymers and chloroform solution of Au nanocrystals. Au nanocrystals are soluble in organic solvent due to their hydrophobic surface, but nanocrystallo-polymers are dissolved in water. (b) The surface tension of aqueous solution of P-*g*-Au NC as a function of concentration.

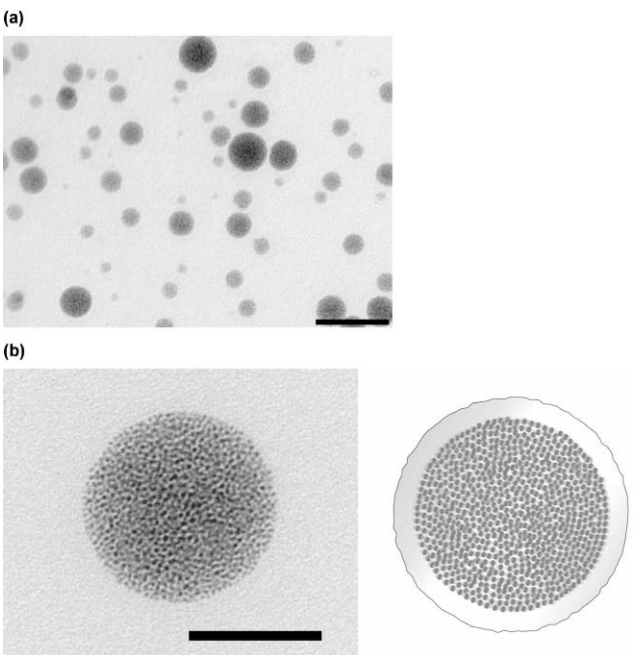

Fig. 3 TEM images of nanocrystallo-spherical aggregates self-assembled from PHEA grafted with Au nanocrystals with DS_{C11SH} of 2.92 mol%. Scale bars: (a) 100 nm; (b) 40 nm.

prepared PHEA grafted with hydrophobic CdSe/ZnS quantum dots with 1.9 nm core diameter and emission wavelength of 490 nm (QD490). The prepared QD490-grafted polymers (P-*g*-QD490) were also amphiphiles with surface-active properties and form spherical self-aggregates (see ESI 4†). The fluorescence behaviour of P-*g*-QD490 that reacts to different environments makes it possible to study the surface-active properties in an obvious and simple way (see ESI 4†). The self-aggregates in aqueous solution have a very low fluorescence emission (approximate wavelength: 490 nm) due to the fluorescence self-quenching of the aggregated QD490s.[26–28] Fluorescence self-quenching is a special instance of static quenching where fluorophores within a critical distance of each other act as perfect traps. However, as chloroform is added to the aqueous solution, the fluorescence intensities gradually increase. The increase of the inter-QD490 distance accompanies the formation of swollen P-*g*-QD490 aggregate because the added chloroform becomes localized in the core of the aggregate and coexists with the QD490s. The result clearly indicates the dynamic self-assembling and surface-active properties of the amphiphilic nanocrystallo-polymers with a controlled arrangement of QD490s.

Fabrication of various nanostructures was achieved by introducing a co-hydrophobic group (Fig. 4). A dodecyl chain, a short hydrophobic carbon chain, was introduced as a co-hydrophobic group to lead the structural transformation by controlling the hydrophilic/hydrophobic ratio of the nanocrystallo-polymer molecules. Recently, our research group reported the aqueous self-assembly behavior of graft copolymers composed of a hydrophilic polymer backbone and grafted hydrophobic compartments, relevant to the amount of grafted hydrophobic chains.[16,29–31] In accordance with the grafted materials and their DS, the formation of various nanostructures, including spherical micelles with various diameters, cylindrical micelles, tubules, and vesicles, was studied.[16,30,31] It was found that dodecyl chains induced a dramatic structural transition while maintaining the water solubility of a polymer material when grafted onto a PHEA backbone over a wide range of DS.[31]

Three P-*g*-$C_{11}SH$-C_{12} polymers with dodecyl chains with different DS (DS_{C12}) and undecanethiols with a fixed DS (DS_{C11SH}) of 3.01 mol% were prepared (Table 1). The introduced dodecyl groups help achieve hydrophobic interactions by contributing to the hydrophobic portion of the

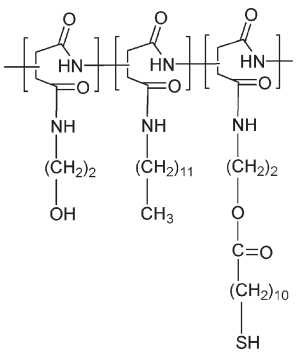

Fig. 4 Chemical structure of PHEA grafted with undecanethiols and dodecyl chains.

nanocrystallo-polymer molecule. Furthermore, they also affect the changing of the overall molecular shape, which is directly relevant to the molecular packing parameter, without molecular steric interference around the Au nanocrystals. Therefore, packing Au nanoparticles into various structures can be realized. With the formation of P-*g*-Au NC-C_{12} polymers by ligand place-exchange, spherical aggregates with a smaller diameter, as well as cylinders, were obtained in the aqueous solution.

Fig. 5a shows the TEM image of the spherical aggregates of P-*g*-Au NC-C_{12} 1 in aqueous solution. Nanocrystallo-spherical aggregates corresponding to those of P-*g*-Au NC but with a slightly smaller diameter (20–50 nm sized Au nanocrystal aggregates) were formed. The reduced mean diameter was also verified by DLS measurement, and the measured D_h of the aggregates was 59.7 nm. The aggregate size tends to decrease as a function of the amount of grafted hydrophobic side chains until the molecular composition approaches the transitional point where the spherical aggregates transform into another structure.[16,30,31] To confirm the morphology of the spherical aggregates, atomic force microscopy (AFM) images of self-aggregates from P-*g*-Au NC-C_{12} 1 were also obtained (see ESI 5†). In the AFM images, spherical shapes of the self-aggregates were found.

P-*g*-Au NC-C_{12} 2, which may have a molecular composition near the transitional point, formed extremely small spherical self-aggregates with a core–shell morphology by allowing only one Au nanocrystal per self-aggregate (Fig. 5b). The core–shell unimolecular micelle solution was negatively stained with phosphotungstic acid solution (2 wt%) because observation of the exact morphology is not possible without staining. Only one Au nanocrystal, with a diameter of 1.5 nm, was embedded in each spherical aggregate with an approximate diameter of 7 nm. Every Au nanocrystal was separated by some distance by being effectively insulated with a polymer shell (inset of Fig. 5b). Beyond the transitional point, nanocrystallo-aggregates with different structures were formed. Fig. 5c shows the TEM images of the negatively stained cylinders obtained from P-*g*-Au NC-C_{12} 3. Entangled and stretched (inset of Fig. 5c) cylinders can be clearly observed. The diameter of the cylinder was approximately 7 nm and the Au nanocrystals were regularly embedded. In the hydrophobic core region of the cylinders, spaces between the Au nanocrystals were filled with dodecyl chains. The observed cylinders have finite size and cylinders longer than a few hundreds of nanometres did not show up in the TEM measurement. It is expected that different sizes could be achieved by varying length and number of conjugated polymers.

In the general morphology control manner of amphiphilic materials, the key factor is the hydrophilic/hydrophobic ratio which is usually achieved by controlling the length of each block in prevalent block copolymer systems.[1–3,29–31] In the present nanocrystallo-polymer system, it was achieved by varying the grafted amount of dodecyl chains in the range of 0 to 24 mole%. The relationship between the hydrophilic/hydrophobic ratios and multiple morphologies of the self-aggregates is expected to be explained by using geometrical aspects and curvatures of the molecules. The length and number of polymers conjugated to a nanocrystal could also be the important factors affecting

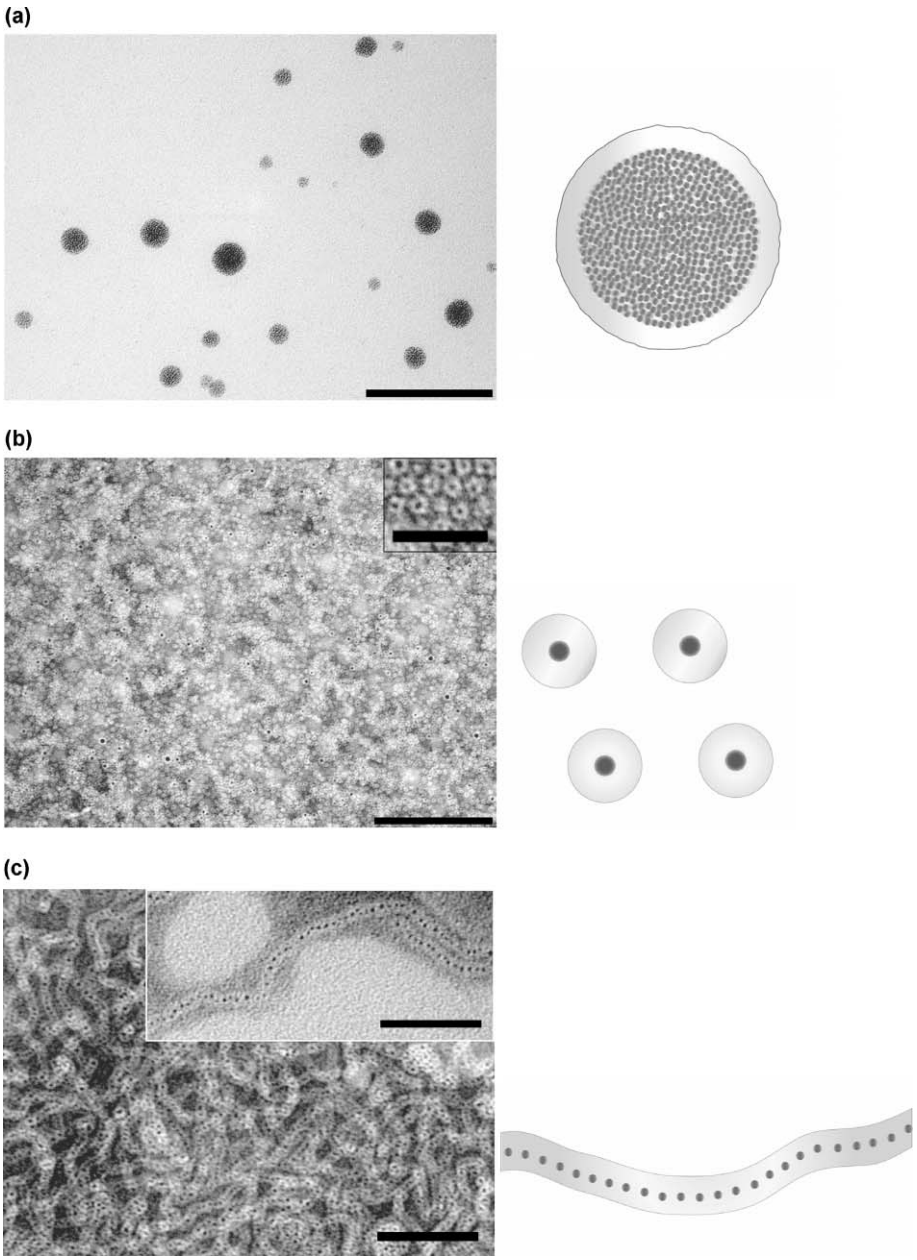

Fig. 5 TEM images of various nanostructures self-assembled from PHEA grafted with Au nanocrystals and dodecyl chains. (a) Spherical aggregates from P-*g*-Au NC-C_{12} 1. (b) Core–shell type unimolecular micelles from P-*g*-Au NC-C_{12} 2. (c) Cylinders from P-*g*-Au NC-C_{12} 3. The samples in (b) and (c) were negatively stained. Scale bars: (a) 200 nm; (b) 200 nm (inset : 40 nm); (c) 80 nm (inset : 40 nm).

geometrical aspects and morphologies of self-aggregates. Further interpretation with some measurable parameters is the subject of our ongoing study.

To confirm and characterize the self-aggregate structures, small angle neutron scattering (SANS) measurements were performed.[32–37] The SANS intensity of 1% (w/v) P-*g*-Au NC aggregates in D_2O is shown in Fig. 6a. Since the difference of Au nanocrystals and organic ligand chains of P-*g*-Au NC is nearly invisible to SANS, P-*g*-Au NC aggregates were modeled as polydisperse core–shell spheres[32,33] to describe all of the aggregated dodecanethiolate-coated Au nanocrystals (core) and PHEA layers (shell). The solid line is the model fit with polydisperse core–shell sphere form factor, which agrees with the SANS intensity very well, resulting in a core radius of R_c = 31.85 nm with a polydispersity of σ = 0.2 and a shell thickness of δ = 3.85 nm (with the scattering length density (SLD) values for each part: $\rho_{media(D2O)} = 6.33 \times 10^{10}$ cm^{-2}, $\rho_{shell} = 1.94 \times 10^{10}$ cm^{-2}, and $\rho_{core} = 5.68 \times 10^{10}$ cm^{-2}).

To ensure the existence of a shell that is invisible in TEM and the overall core–shell structure, a neutron contrast matching experiment was performed. When the SLD of the core was matched by mixing D_2O and H_2O with an appropriate ratio, the aggregates could be considered as a polydisperse hollow sphere model.[34] Fig. 6b shows the SANS intensity of 1% (w/v) P-*g*-Au NC aggregates in the D_2O–H_2O mixture. The SANS intensity showed the characteristic q^{-2} behavior induced by layer structure and was successfully analyzed using a hollow sphere model with a core radius of

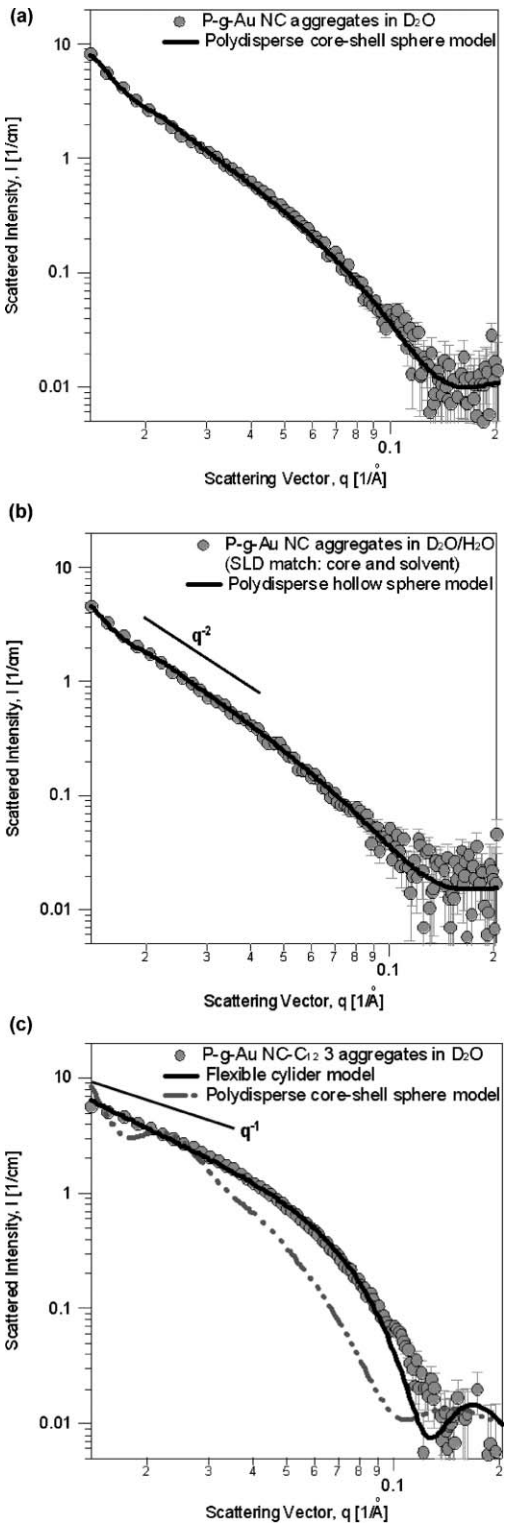

Fig. 6 SANS results of the nanostructures self-assembled from Au nanocrystallo-polymers. (a) SANS experimental data of P-*g*-Au NC in D_2O and fitted curve with polydisperse core–shell model. (b) SANS experimental data of P-*g*-Au NC in D_2O–H_2O mixture (neutron contrast matching with core) and fitted curve with polydisperse hollow sphere model. (c) SANS experimental data of P-*g*-Au NC-C_{12} 3 in D_2O and fitted curves with flexible cylinder model and polydisperse core-shell model.

R_c = 32.08 nm with a polydispersity of σ = 0.2 and a shell thickness of δ = 3.65 nm (with the SLD values for each part: $\rho_{media(D2O/H2O)} = 5.68 \times 10^{10}$ cm^{-2}, $\rho_{shell} = 1.94 \times 10^{10}$ cm^{-2}, and $\rho_{core} = 5.68 \times 10^{10}$ cm^{-2}). The results from two different types of SANS experiments for one sample, P-*g*-Au NC, were almost identical. Therefore, P-*g*-Au NC aggregate structures are verified as 71.43 $\pm$ 0.33 nm sized spherical micellar aggregates composed of a 3.75 $\pm$ 0.1 nm thick hydrophilic PHEA shell and a 63.93 $\pm$ 0.23 nm sized core of tightly aggregated Au nanocrystals.

The SANS intensity of 0.5% (w/v) P-*g*-Au NC-C_{12} 3 aggregates in D_2O are shown in Fig 6c. The SANS intensity shows q^{-1} behavior at the low q region which is typical for the cylinder particle and was successfully analyzed using a flexible cylinder model[35] with a contour length of L = 158.73 nm, a Kuhn length of b = 19.61 nm, and a radius of R = 2.99 nm (with a scattering contrast of $\Delta\rho = 3.92 \times 10^{10}$ cm^{-2}). The slight deviation at a high q region might have been induced by the discrete existence of Au nanocrystals along the middle of the cylinders.

To confirm the model fitting analysis, we attempted to fit the SANS intensity with the polydisperse core–shell model. However, they did not match as shown in Fig. 6c, which means that the Au nanocrystallo-polymer did not form spherical micelles at this point due to the increased hydrophobic/hydrophilic ratio with the introduction of dodecyl chains as co-hydrophobic parts. We found that P-*g*-Au NC-C_{12} 3 forms worm-like cylindrical micelles with an average length of 158.73 nm and diameter of 5.98 nm. The structural characterization results for P-*g*-Au NC aggregates and P-*g*-Au NC-C_{12} 3 aggregates based on different experiments including DLS, TEM, and SANS are reasonably close.

Conclusions

In summary, we fabricated a series of nanocrystallo-polymers. Through the conjugation of Au nanocrystal-linkable side chains and by varying the amount of grafted dodecyl groups, it is possible to incorporate bulky Au nanocrystals and simultaneously control the nanostructures of the self-aggregates from spherical aggregates to cylinders. The self-assembled nanostructures were reproducibly produced and stable against lyophilization–redissolution. This nanocrystallo-polymer system with remarkable structural controllability and dynamic self-assembling and surface-active properties is a breakthrough in recent attempts to assemble nanoparticles. These nanostructures are expected to exhibit new physical properties induced from the conjugated nanocrystals' characteristic properties that bridges molecular and bulk.

Experimental

Preparation of nanocrystallo-spherical aggregates from P-*g*-C_{11}SH, P-*g*-C_{12}-C_{11}SH 1, and P-*g*-C_{12}-C_{11}SH 2

20 mg of each precursor polymer were dissolved in 3 mL of DDI water, and 7 mg of Au nanocrystals or CdSe/ZnS QD were dissolved in 0.6 mL of THF. The nanocrystal–THF solution was added dropwise to the polymer–water solution under vigorous stirring. The mixture was stirred continuously for 24 hours for ligand place exchange. Then, it was dialyzed

against the DDI water to complete the aggregate formation by removing the THF. The unreacted nanocrystals were separated by centrifugation and the nanocrystallo-aggregates in aqueous media were obtained.

Preparation of nanocrystallo-cylinders from P-*g*-C_{12}-C_{11}SH 3

The above method was modified slightly to be more suitable for the altered physicochemical properties of precursor polymers, P-*g*-C_{11}SH-C_{12} 3, by the changed molecular composition. 12 mg of the polymer and 4 mg of Au nanocrystal were dissolved together in 0.4 mL of mixture solvent (THF : DMAc (dimethylacetamide) = 3 : 1). The solution was stirred continuously for 24 hours for ligand place exchange and then added dropwise to 4 mL of the DDI water under vigorous stirring. After 20 minutes of stirring, the mixture solution was dialyzed against the DDI water. After separating the unreacted Au nanocrystals, the nanocrystallo-cylinders in aqueous media were obtained.

SANS experiments

SANS measurements were performed on a 9 m SANS instrument at HANARO (Highflux Advanced Neutron Application Reactor) in KAERI (Korea Atomic Energy Research Institute). Neutrons of wavelength λ = 6.38 Å with full width half-maximum $\Delta\lambda/\lambda$ = 11% were used. The sample to detector distance (3.0 m) was used to cover a q-range of 0.008–0.02 $Å^{-1}$ where $q = 4(\pi/\lambda)\sin(\theta/2)$ is the magnitude of the scattering vector and θ is the scattering angle. Sample scattering was corrected for background and empty cell scattering. The corrected data sets were placed on an absolute scale using standard samples.

SANS data analysis

In the particulate system, the scattering intensity of particles can be written as

$$I(q) = (\Delta\rho)^2 n_p P(q) S(q) + bkg$$

where $\Delta\rho$ is the contrast of the SLD between the particles and media, n_p is the number density of particles, $P(q)$ is an intraparticle interference term (form factor), $S(q)$ is an interparticle interference term (structure factor), and bkg is the residual incoherent scattering. For very dilute solutions of particles where the interparticle interference is negligible, the scattering intensity can be simplified as

$$I(q) = (\Delta\rho)^2 n_p P(q) + bkg.$$

SANS data sets were analyzed by model fit. For the spherical micelle-like aggregates, the core–shell model and the hollow sphere model were considered and the Schulz distribution function was introduced for the polydispersity. The core–shell model is described as

$$(\Delta\rho)^2 P(q) = \left[\frac{3V_c(\rho_c-\rho_s)j_1(qR_c)}{qR_c} + \frac{3V_s(\rho_s-\rho_{solv})j_1(qR_s)}{qR_s}\right]^2$$

$$j_i(x) = (\sin x - x\cos x)/x^2$$

where V_c and V_s are the volume of core and shell, R_c and R_s are the radii of core and shell, and ρ_c, ρ_s, and ρ_{solv} are the SLDs of core, shell and solvent, respectively. $j_1(x)$ is the first-order spherical Bessel function. The form factor was normalized with the width parameter of the Schulz distribution, z, which is given as $z = (1/p^2) - 1$ where p is the polydispersity (= σ/R_c). In the hollow sphere model ρ_c becomes the same as ρ_{solv}.

For the cylindrical micelle, the flexible cylinder model was considered.

$$I_{WC}(q,L,b,R_{CS}) = c\Delta\rho_m{}^2 M S_{WC}(q,L,b) P_{CS}(q,R_{CS}) + bkg$$

where L is the contour length, b is the Kuhn length, R_{CS} is the circular cross sectional radius, c is the concentration, M gives the average molecular weight of micelle, $S_{WC}(q,L,b)$ is the scattering function of a single semiflexible chain with excluded volume effects and $P_{CS}(q,R_{CS})$ is the scattering function from the cross section of a rigid rod.

$$P_{CS}(q,R_{CS}) = \left[\frac{2j_1(qR_{CS})}{qR_{CS}}\right]^2$$

$$S_{WC}(q,L,b) = [1-w(qR_g)]S_{Debye}(q,L,b) + w(q,R_g)\left[1.22(qR_g)^{-1/0.585} + 0.4288(qR_g)^{-2/0.585} - 1.651(qR_g)^{-3/0.585}\right] + \frac{C(n_b)}{n_b}\left\{\frac{4}{15} + \frac{7}{15u} - \left(\frac{11}{15} + \frac{7}{15u}\right)\times\exp[-u(q,L,b)]\right\}$$

where R_g is the radius of gyration with excluded volume effects and $w(qR_g)$ is an empirical crossover function chosen as:

$$w(x) = \frac{\{1+\tanh[(x-1.523)/0.1477]\}}{2}$$

$$n_b = \frac{L}{b}$$

For $L > 10b$, $C(n_b) = 3.06{n_b}^{-0.44}$ and for $L \leqslant 10b$, $C(n_b) = 1$. S_{Debye} is the Debye function with $u = \langle R_g{}^2\rangle q^2$.

$$S_{Debye}(q,L,b) = \frac{2}{u(q,L,b)}\{\exp[-u(q,L,b)] + u(q,L,b) - 1\}$$

$$u(q,L,b) = \frac{Lb}{6}\left\{1 - \frac{3}{2n_b} + \frac{3}{2n_b^2} + \frac{3}{4n_b^3}[1-\exp(-2n_b)]\right\}q^2$$

$$\langle R_g^2\rangle = \alpha(n_b)^2\frac{bL}{6}$$

$$u(q,L,b) = \alpha(n_b)^2\frac{bL}{6}q^2$$

where $\alpha(n_b)$ is the expansion factor which follows the following empirical expression:

$$\alpha(x) = \sqrt{\left[1 + \left(\frac{x}{3.12}\right)^2 + \left(\frac{x}{8.67}\right)^3\right]^{0.176/3}}$$

Acknowledgements

This work was supported by the Eco-Technopia 21 Project (Ministry of Environment), the Nano R&D Program (Ministry of Science and Technology), and the HANARO Utilization Project (Ministry of Science and Technology) of the Korean government. We thank the staff of Chuncheon KBSI for their assistance with the TEM measurements.

References

1 L. Zhang and A. Eisenberg, *Science*, 1995, **268**, 1728–1731.
2 J. J. L. M. Cornelissen, M. Fischer, N. A. J. M. Sommerdijk and R. J. M. Nolte, *Science*, 1998, **280**, 1427–1430.
3 E. G. Bellomo, M. D. Wyrsta, L. Pakstis, D. J. Pochan and T. J. Deming, *Nat. Mater.*, 2004, **3**, 244–248.
4 B. G. G. Lohmeijer and U. S. Schubert, *Angew. Chem., Int. Ed.*, 2002, **41**, 3825–3829.
5 D. Domínguez-Gutiérrez, M. Surtchev, E. Eiser and C. J. Elsevier, *Nano Lett.*, 2006, **6**, 145–147.
6 H. Ai, C. Flask, B. Weinberg, X. Shuai, M. D. Pagel, D. Farrell, J. Duerk and J. Gao, *Adv. Mater.*, 2005, **17**, 1949–1952.
7 H. Fan, E. W. Leve, C. Scullin, J. Gabaldon, D. Tallant, S. Bunge, T. Boyle, M. C. Wilson and C. J. Brinker, *Nano Lett.*, 2005, **5**, 645–648.
8 Z. Zhang, M. A. Horsch, M. H. Lamm and S. C. Glotzer, *Nano Lett.*, 2003, **3**, 1341–1346.
9 C. R. Iacovella, M. A. Horsch, Z. Zhang and S. C. Glotzer, *Langmuir*, 2005, **21**, 9488–9494.
10 A. K. Boal, F. Ilhan, J. E. DeRouchey, T. Thurn-Albrecht, T. P. Russell and V. M. Rotello, *Nature*, 2000, **404**, 746–748.
11 A. K. Boal, B. L. Frankamp, O. Uzun, M. T. Tuominen and V. M. Rotello, *Chem. Mater.*, 2004, **16**, 3252–3256.
12 E. R. Zubarev, J. Xu, A. Sayyad and J. D. Gibson, *J. Am. Chem. Soc.*, 2006, **128**, 4958–4959.
13 E. R. Zubarev, J. Xu, A. Sayyad and J. D. Gibson, *J. Am. Chem. Soc.*, 2006, **128**, 15098–15099.
14 S. R. Yang, J. H. Jeong, K. Park and J.-D. Kim, *Colloid Polym. Sci.*, 2003, **281**, 852–861.
15 H. Kang, J.-D. Kim, S.-H. Han and I.-S. Chang, *J. Controlled Release*, 2002, **81**, 135–144.
16 H. S. Kang, S. R. Yang, J.-D. Kim, S.-H. Han and I.-S. Chang, *Langmuir*, 2001, **17**, 7501–7506.
17 M. Brust, M. Walker, D. Bethell, D. J. Schiffrin and R. J. Whyman, *J. Chem. Soc., Chem. Commun.*, 1994, 801–802.
18 M. Brust, J. Fink, D. Bethell, D. J. Schiffrin and C. J. Kiely, *J. Chem. Soc., Chem. Commun.*, 1995, 1655–1656.
19 M. J. Hostetler, J. E. Wingate, C. J. Zhong, J. E. Harris, R. W. Vachet, M. R. Clark, J. D. Londono, S. J. Green, J. J. Stokes, G. D. Wignall, G. L. Glish, M. D. Porter, N. D. Evans and R. W. Murray, *Langmuir*, 1998, **14**, 17–30.
20 M.-C. Daniel and D. Astruc, *Chem. Rev.*, 2004, **104**, 293–346.
21 A. C. Templeton, M. J. Hostetler, C. T. Kraft and R. W. Murray, *J. Am. Chem. Soc.*, 1998, **120**, 1906–1911.
22 M. J. Hostetler, A. C. Templeton and R. W. Murray, *Langmuir*, 1999, **15**, 3782–3789.
23 M. J. Hostetler, S. J. Green, J. J. Stokes and R. W. Murray, *J. Am. Chem. Soc.*, 1999, **118**, 4212–4213.
24 A. C. Templeton, W. P. Wuelfing and R. W. Murray, *Acc. Chem. Res.*, 2000, **33**, 27–36.
25 T. Pham, J. B. Jackson, N. J. Halas and R. Lee, *Langmuir*, 2002, **18**, 4915–4920.
26 Z. Tang, Z. Zhang, Y. Wang, S. C. Glotzer and N. A. Kotov, *Science*, 2006, **314**, 274–278.
27 C. R. Kagan, C. B. Murray, M. Nirmal and M. G. Bawendi, *Phys. Rev. Lett.*, 1996, **76**, 1517–1520.
28 S. A. Crooker, J. A. Hollingsworth, S. Tretiak and V. I. Klimov, *Phys. Rev. Lett.*, 2002, **89**, 186802.
29 J. H. Jeong, H. S. Kang, S. R. Yang and J.-D. Kim, *Polymer*, 2003, **44**, 583–591.
30 H. J. Lee, S. R. Yang, E. J. An and J.-D. Kim, *Macromolecules*, 2006, **39**, 4938–4940.
31 E. J. An, H. J. Lee, K.-S. Jang, J.-Y. Kim and J.-D. Kim, *Macromolecules*, to be submitted.
32 J.-B. Jeong, S. R. Yang and J.-D. Kim, *Langmuir*, 2002, **18**, 8749–8755.
33 S. H. Choi, J.-H. Lee, S.-M. Choi and T. G. Park, *Langmuir*, 2006, **22**, 1758–1762.
34 H. Kukula, H. Schlaad, M. Antonietti and S. Förster, *J. Am. Chem. Soc.*, 2002, **124**, 1658–1663.
35 W.-R. Chen, P. D. Butler and L. J. Magid, *Langmuir*, 2006, **22**, 6539–6548.
36 T.-H. Kim, S.-M. Choi and S. R. Kline, *Langmuir*, 2006, **22**, 2844–2850.
37 T.-H. Kim, C. Doe, S. R. Kline and S.-M. Choi, *Adv. Mater.*, 2007, **19**, 929–933.

